Fixation of Nanosized Proton Transport Channels in Membranes†

Jongok Won,*,‡ Hye Hun Park,§ Young Jin Kim,§ Sang Wook Choi,§ Heung Yong Ha,§ In-Hwan Oh,§ Hoon Sik Kim,§ Yong Soo Kang,§ and Kyo Jin Ihn⊥

Department of Applied Chemistry, Sejong University, 98 Gunja, Gwangjin, Seoul, 143-747, Korea; Korea Institute of Science and Technology, P.O. Box 131 Cheongryang, Seoul 130-650 Korea; and Department of Chemical Engineering, Kangwon National University, 192-1, Hyoja2, Chunchon, Kangwon, 200-701, Korea

Received January 5, 2003; Revised Manuscript Received March 12, 2003

ABSTRACT: The structure of proton transport channels is controlled and fixed in sulfonated poly(styrene-*b*-butadiene-*b*-styrene) (SBS) triblock copolymer membranes. Microphase-separated SBS membranes were cross-linked by UV irradiation in the presence of a photoinitiator and then sulfonated by acetyl sulfate. Sulfonated cross-linked SBS (scSBS) membranes with fixed nanosized proton transport channels were then prepared. The scSBS membranes show good proton conductivity, comparable to that of Nafion, and a low methanol permeability, more than 1 order of magnitude smaller than that of Nafion. Sulfonated non-cross-linkable poly(styrene-*b*-(ethylene-*r*-butylene)-*b*-styrene) membranes and sulfonated cross-linked poly(styrene-*r*-butadiene) membranes, which have less developed proton transport channels, were also prepared for comparison. The effects of the presence and size of the proton transport channels on the proton conductivity and methanol permeability were investigated. It is concluded that both the structure and the fixation of the proton transport channels are crucial to the functioning of proton exchange membranes of direct methanol fuel cells.

1. Introduction

Direct methanol fuel cells (DMFCs) are promising candidates for portable power sources and transport applications because they do not require the fuel processing equipment (such as reformers or catalytic burners) that is essential for polymer electrolyte membrane fuel cells (PEMFCs) and they can be operated at low temperatures.[1] A DMFC consists of a proton-exchange membrane sandwiched between an anode and a cathode. The proton-exchange membrane requires three major functions: as a proton conductor, as a fuel barrier, and as a mechanical separator between the two electrodes.

The membranes commonly used in current DMFCs were originally developed for PEMFC applications[2,3] and typically have a phase-separated structure comprising a hydrophobic matrix and interconnected hydrophilic clusters, called ionic channels. Proton conduction occurs through the ionic channels of the membranes;[4] these channels are formed by micro- or nanophase separation between the hydrophilic proton exchange sites and the hydrophobic domain, as observed for instance in perfluorosulfonic acid (Nafion, DuPont) and sulfonated poly(styrene-*b*-(ethylene-*r*-butylene)-*b*-styrene) copolymers (sSEBS, DAIS). The drawback of the use in DMFCs of membranes developed for PEMFCs is that they are not optimal with regard to methanol blocking because methanol can be transported across the membrane to the cathode, known as methanol crossover. This process occurs due to the similarity between methanol's properties and those of water (e.g., dipole moment).[5,6] For example, Nafion exhibiting a phase-separated morphology has a high proton conductivity, but it has been found that over 40% of the methanol can be lost in DMFC across such membranes due to the swelling of the membrane.[7] Therefore, methanol crossover needs to be reduced, while maintaining proton conductivity and mechanical strength, to improve fuel cell performance.

It is known that methanol primarily permeates the membranes through ionic channels, and thus the cross-sectional size of these channels determines methanol permeability. This size is, in turn, depended by the "swellability" of the membrane. Thus, swelling facilitates the permeation of both methanol and water as well as that of protons to some extent.[7,8] Therefore, swellability also needs to be reduced while maintaining high proton conductivity and mechanical strength to obtain low methanol permeability; this can be achieved by controlling the structure of the ionic channels.

Manipulating block copolymers is a popular method for controlling the structure of the phase-separated microdomains of the matrix. Partially sulfonated SEBS triblock copolymers and sulfonated poly(styrene-*r*-butadiene) (SBR) copolymers have the advantages of ease of morphology control and low cost and hence have been widely studied.[9−14] SBR was hydrogenated first to avoid possible cross-linking/cyclization and to improve chemical stability during sulfonation. SEBS and hydrogenated SBR were subsequently sulfonated on its styrene units,[13,15−17] as shown in Scheme 1a. Several investigations have studied the morphology and the chemical and physical properties of sSEBS membranes.[10,18,19] The mechanical strength of sSEBS membranes is closely associated with the extent of physical cross-linkage between the ethylene/butylene domains, but this physically cross-linked structure can become disentangled in water and, to an even greater extent, in methanol, resulting in large swelling as shown in Scheme 1a. This swelling-induced disentanglement behavior is the main reason for the enlargement of the ionic channels and

† Presented at the IUPAC-PC2002, Kyoto, Japan, Dec 2002.

‡ Sejong University.
§ Korea Institute of Science and Technology.
⊥ Kangwon National University.
* To whom correspondence should be addressed: Tel +82-2-3408-3230; Fax +82-2-462-9954; e-mail jwon@sejong.ac.kr.

10.1021/ma034014b CCC: $25.00 © 2003 American Chemical Society
Published on Web 04/08/2003

Scheme 1

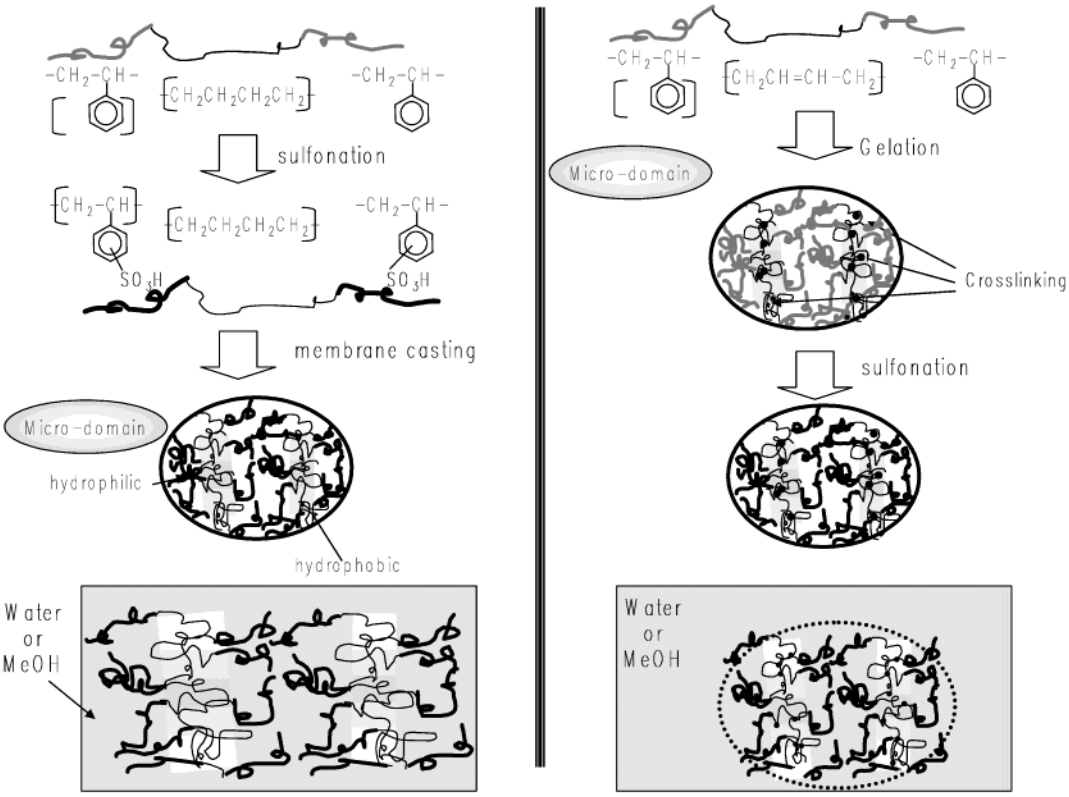

(a) non-crosslinkable sSEBS (b) Crosslinked sSBS

consequently for the observed methanol crossover phenomena. Therefore, it is also necessary to reduce swellability by fixing the microdomain structure of the membrane.

A common method for fixing membrane morphology is to cross-link polymeric chains of the hydrophobic matrix by UV irradiation.[20−22] Here, we have chosen poly(styrene-*b*-butadiene-*b*-styrene) (SBS) triblock and SBR copolymers because they contain reactive double bonds readily cross-linkable by UV irradiation,[23−26] which can then be subsequently sulfonated to various extents (Scheme 1b). The extent of sulfonation was carefully controlled so as to maximize the proton conductivity. The SBS membrane has a microphase-separated structure while the SBR membrane has a relatively homogeneous random structure. The effects of these differences in structure, particularly of the ionic channel structure, on proton and methanol permeabilities are investigated in this study by assessing the membranes' performances and characterizing their structures.

2. Experimental Section

2.1. Materials. Poly(styrene-*b*-butadiene-*b*-styrene) (SBS) ($M_w \sim 140\,000$; 30 wt % styrene; Aldrich) and poly(styrene-*r*-butadiene) random copolymer (SBR) ($M_w \sim 1\,000\,000$; 45 wt % styrene; Scientific Polymer Products, Inc.) were purchased and purified by precipitation in order to remove the stabilizer. Sulfonated poly(styrene-*b*-(ethylene-*r*-butylene)-*b*-styrene) (sSEBS) solution in 1-propanol and dichloroethane ($M_w \sim 80\,000$; 28 wt % styrene and 45% of sulfonation; Aldrich) was used as received. The photoinitiator, 2,4,6-trimethylbenzoyl-diphenylphosphine oxide (Lucirin TPO from BASF), was kindly provided by BASF Korea Co. H_2SO_4 (95%, Daejung), acetic anhydride (Daejung), toluene (Aldrich), 1,2-dichloroethane (DCE: Junsei), and methanol (Merck) were used as received.

2.2. Preparation of Membranes. A solution of 5 wt % SBS in toluene with 5 wt % of the photoinitiator of SBS was prepared and filtered. The concentration of the photoinitiator was chosen according to procedures specified in a previous report.[24] The solution was poured into a glass dish and held at room temperature until complete evaporation of the solvent had taken place. The residual solvent was evaporated under vacuum. Membrane thickness was measured using a digital micrometer. Both sides of the samples were exposed to irradiation of 1700 μW/cm^2 for 120 min in a UV cross-linker (Spectrolinker XL-1000, Spectronics Co., New York) to obtain cross-linked SBS (cSBS) films. From quantitative ^{13}C NMR spectral analysis, it has been shown that SBS films have butadiene blocks containing 60.5%, 29.5%, and 10% of *trans*-1,4-, *cis*-1,4-, and vinyl isomeric units, respectively.[26] It is assumed that cross-linking mainly occurred in the butadiene phase.

cSBS films can be sulfonated using acetyl sulfate.[17,27] The appropriate amount of acetic anhydride in DCE was cooled below 0 °C, and the corresponding volume of sulfuric acid was added. The acetyl sulfate solution was maintained at 0 °C in an ice bath until its addition to the reaction medium. The cSBS film was swollen in an excess amount of DCE overnight. The solution was heated to 50 °C and purged with nitrogen for 30 min. Then the acetyl sulfate solution (produced with the procedure described above) was added. Different mole ratios of acetyl sulfate to phenyl groups ($[CH_3CO_2SO_3H]/[C_6H_5]$) in the range 0.01−2 were used. Fresh acetyl sulfate was prepared prior to each sulfonation reaction. The solution was stirred for 4 h at this temperature, and then the reaction was terminated by the addition of 2-propanol, resulting in a sulfonated SBS cross-linked membrane (scSBS). The membrane was washed in boiling water and many times with cold water. The complete removal of residual acid from the final product after sulfonation is important since it can interfere with the properties of the final product.

The importance of the membrane structure and of the fixation of the proton transport channels of the scSBS membranes was studied through comparison with the following systems.

Table 1. Characterization of the Membranes

ID	molar feed ratio[a] (m/m)	thickness (μm)	degree of sulfonation (%)	proton conductivity (S/cm)	methanol permeability (cm^2/s)	Φ
scSBS1	1	88.2	$15._8$	7.1×10^{-5}	*b*	
scSBS1.5	1.5	88.6	$23._5$	6.1×10^{-3}	*b*	
scSBS2	2	76.0	$36._8$	2.3×10^{-2}	8.1×10^{-8}	280 000
scSBR1	1	166	7.0	2.7×10^{-8}	*b*	
scSBR1.5	1.5	92	$31._6$	6.5×10^{-6}	*b*	
scSBR2	2	132	$40._2$	1.5×10^{-5}	*b*	
scSBR2.5	2.5	115	$51._4$	1.9×10^{-5}	7.4×10^{-8}	260
Nafion 117		170		6.3×10^{-2}	2.9×10^{-6}	22 000
sSEBS		90	45	3.8×10^{-2}	1.7×10^{-6}	22 000

[a] Molar feed ratio; $[CH_3CO_2SO_3H]/[C_6H_5]$. [b] No detection.

Structure Fixation. Non-cross-linkable sSEBS film was prepared by pouring sSEBS stock solution into a glass dish and drying it at room temperature until complete evaporation of the solvent had taken place.

Structure Formation. Sulfonated cross-linked SBR films (scSBR) do not have a distinct phase-separated structure like that of scSBS films. A 5 wt % SBR solution in toluene containing the photoinitiator Lucirin TPO was poured into a glass dish and placed at room temperature until complete evaporation of the solvent had occurred. The resulting SBR film was then cross-linked by UV irradiation and sulfonated by acetyl sulfate with the same procedure as used for the scSBS membrane.

2.3. Characterization. Thin films of the membranes were prepared on a KBr crystal for FT-IR analysis. Measurements were performed on a 6030 Galaxy Series FT-IR spectrometer (Mattson Instruments); 256 scans were signal-averaged at a resolution of 4 cm^{-1}. The degree of sulfonation was determined by elemental analysis and characterized by FT-IR.

The swelling characteristics of the membranes were determined by water or solvent uptake measurements. The samples were dried under vacuum for 24 h at 30 °C and then weighed. They were then placed in deionized water for a week at 25 °C. Before sample weighing, the excess water or solvent on the membrane surface was removed with absorbent paper. The water uptake content was calculated using the following relationship:

$$\text{water uptake content (\%)} = \frac{M_{\text{wet}} - M_{\text{dry}}}{M_{\text{dry}}} \times 100 \quad (1)$$

where M_{wet} and M_{dry} are the weights of the wet and dried samples, respectively.

A four-point probe method was used to measure the proton conductivity of the membranes. Before the measurement of proton conductivity, the prepared membranes were equilibrated with deionized water. Complex impedance measurements were carried out in the frequency range 1 Hz−8 MHz at 25 °C, using a ZAHNER IM-6 impedance analyzer.[28] The impedance spectra of the membranes can be used to generate Nyquist plots,[29,30] and the proton conductivity was calculated from the plots.[28]

The methanol permeability of the membranes was determined using a diffusion cell described in the literature.[31−33] This cell consists of two reservoirs, each approximately 48 mL, separated by a vertical membrane. Each membrane is clamped between the two reservoirs and stirred during the experiment. Prior to testing, the membranes were equilibrated in deionized water for at least 24 h. Initially, one reservoir contains a methanol−water mixture (10 wt % methanol) and the other reservoir only contains water. Increases of the concentration of methanol in the water reservoir with time were detected by gas chromatography (Gow-Mac Instrument Co.) and with a differential refractometer (RI750F by Young In Co.). Each reservoir has a capillary tube for sampling l μL for gas chromatography.[33,34] The uncertainty of the obtained values was less than 2%.

Synchrotron small-angle X-ray scattering (SAXS) measurements were performed at the 4C1 SAXS beamline at the Pohang Accelerator Laboratory, Korea. The raw data were corrected for scattering from the empty cell, for air scattering, for dark current from the detector, and for sample transmission. Following these corrections, the data were circularly averaged to produce $I(q)$ vs q plots where $I(q)$ is the scattered intensity and q is the scattering vector related to the scattering angle 2θ ($q = 4\pi \sin\theta/\lambda$). The typical beam size was less than 1×1 mm^2, and the q range was 0.007 to 0.139 $Å^{-1}$. Measurements were carried out for samples in both the dried and water-swollen states. All samples were kept in sealed polyimide envelopes during the measurements.

Ultrathin sections of the samples were prepared in order to observe their morphology. Sample films were imbedded into an epoxy resin, Epon-812, purchased from SPI. Ultrathin cross sections of the films of approximately 90 nm thickness were prepared at −90 °C by an ultramicrotome of model Ultracut-R made by Leica using a diamond knife. The thin-sectioned films were mounted on a copper grid and stained with OsO_4 vapor. Carbon was evaporated onto the specimens in order to prevent accumulation of electrons during TEM observation. Transmission electron microscopy was performed at 200 kV by a JEOL TEM, model JEM-2010.

3. Results and Discussion

Membrane Characterization. The SBS films became insoluble in DCE upon irradiation in the presence of photoinitiator. On the other hand, SBS films were found to remain soluble in DCE when exposed to UV irradiation in the absence of the photoinitiator under the same conditions. The photoinitiated reactions of the vinyl double bonds located on different polybutadiene blocks lead to the formation of a three-dimensional polymer network, which accounts for the observed insolubility in DCE of the UV-irradiated SBS films.

The IR spectra show that after cross-linking a small decrease in the height of the peaks due to the vinyl double bonds at 972.6 and 1637.5 cm^{-1} is observed, which is in agreement with previous results.[24,35,36] The size of this decrease suggests that only minimal cross-linking occurs in the SBS film upon UV exposure. The cSBS film remained insoluble with no loss of shape in all solvents tested, implying that there are enough cross-linkages to hold the structure. The degree of swelling of the cSBS film in DCE was ca. 200%, suggesting a fairly loose structure as is important for the subsequent sulfonation reaction. The polystyrene segments of the SBS block copolymer are not expected to participate in the cross-linking process, but side reactions may occur if some propagating radicals abstract labile hydrogen atoms from PS chains.

We prepared SBS block and SBR random copolymer membranes with various degrees of sulfonation. Their characteristics are presented in Table 1 along with those of the Nafion 117 and sSEBS membranes for comparison. The extent of sulfonation was controlled by varying the molar ratio of acetyl sulfate to phenyl groups [CH_3-

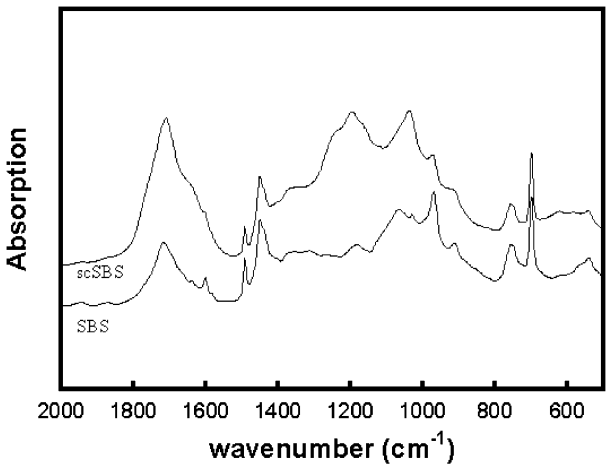

Figure 1. FT-IR spectra of SBS and scSBS samples.

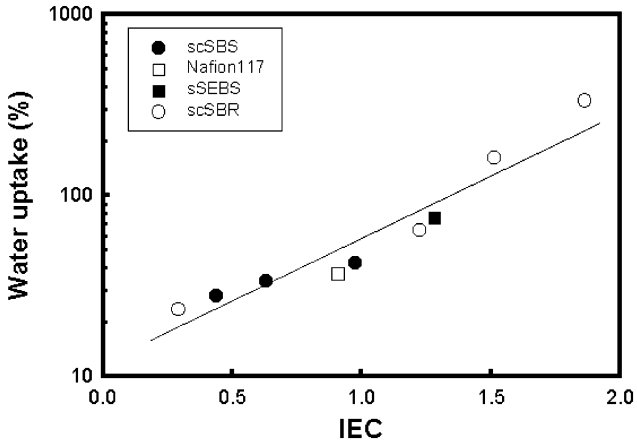

Figure 2. Water uptake contents of the samples as a function of IEC.

$CO_2SO_3H]/[C_6H_5]$. The FT-IR spectra of the cSBS and scSBS membranes are shown in Figure 1. The success of the sulfonation reaction was confirmed by detection of an absorbance peak around 1238 cm^{-1}, which is due to the asymmetric stretching vibrations of sulfonate groups.[14]

From the elemental analysis, it was found that the degree of sulfonation changed from 16 to 37% when the molar feed ratio of $[CH_3CO_2SO_3H]/[C_6H_5]$ was increased from 1 to 2. In practice, the resulting concentration of sulfonate groups in the polymer is significantly lower than the feed concentration. This is because the reaction is taking place in the solid state of the membrane. In the solid state, chain mobility is very limited, resulting in a low reaction yield. However, in this system, the cSBS membrane is swollen by up to 200%, which permits some chain mobility, and thus the sulfonation reaction can occur.

The water uptake content of the membranes in water are plotted with respect to averaged ion-exchange capacity (IEC) in Figure 2. The IEC is calculated as the quotient of the molar content of the sulfonate groups and the membrane weight. The degree of swelling in water increases with the concentration of ionic sites, i.e., of sulfonic acid groups. Since scSBS and sSEBS are sulfonated "block" copolymers, while Nafion and sSBR are sulfonated "random" copolymers, they may have different microdomain structures. However, as can be seen in the figure, the degree of swelling depends only on the IEC values of the membranes and is independent of the structures of their microdomains.

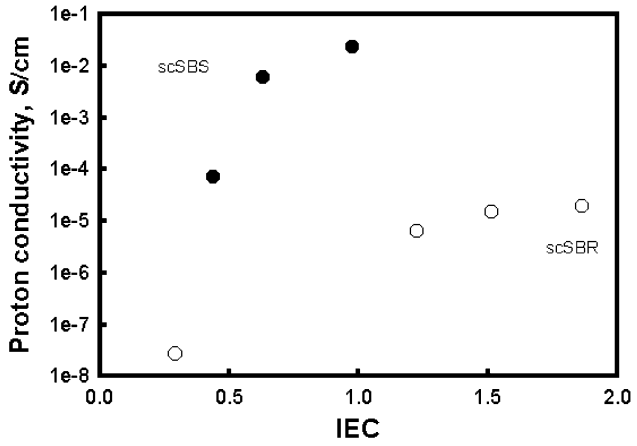

Figure 3. Proton conductivity of the samples as a function of IEC.

The proton conductivities of the sulfonated polymers were determined by impedance spectroscopy and plotted in Figure 3. The proton conductivity increased with IEC, that is, with the degree of sulfonation. It is generally known that the ionic conductivity and the degree of swelling of a membrane increase with the concentration of ionic sites for a given membrane structure.[37] However, Figure 3 clearly shows that there is also a strong dependence of the proton conductivity on the microdomain structure. The scSBS membrane has a phase-separated structure while the scSBR membrane has a relatively homogeneous structure. This suggests that the ionic conductivity strongly depends on both the degree of sulfonation and the membrane microstructure, while the degree of swelling depends only on the degree of sulfonation. For example, in the cases of scSBR1.5 and scSBS2, the former swells to twice the degree of the latter, but the former exhibits 3 orders of magnitude less proton conductivity than the latter. It is concluded that increases in the degree of sulfonation are essential for improving ionic conductivity[38] and that the microstructure also plays a crucial role in determining the ionic conductivity. These structural effects are discussed in more detail in the next section.

In Table 1, the permeances of 10 wt % methanol through the various membranes are given. It is clear that the cross-linked sulfonated membrane has low methanol permeability. The scSBS2 membrane has a methanol permeability 1 order of magnitude less than those of the Nafion or sSEBS membranes, while its proton conductivity is comparable to those of the Nafion or sSEBS membranes. Maintenance of the size of the ionic channels by permanent cross-linkages may be the main reason for this low methanol permeability; the methanol permeability may be reduced because of the reduced size of the ionic channel.

Structural Characterization. SAXS was used to study the size and the spatial arrangement of the microdomains of the block copolymers. Typical SAXS data for the pristine SBS, cSBS, and scSBS1.5 films in both dried and water-swollen states are shown in Figure 4. The microdomain morphology of a block copolymer can be determined from the q values of higher-order peaks relative to the first-order peak for interparticle scattering because such materials exhibit different arrays depending on the dominant shapes of their microdomain structures, such as spheres in a cubic lattice, cylinders in a hexagonal lattice, and lamellar arrangements.[39−41] Cylinders arranged in a hexagonal

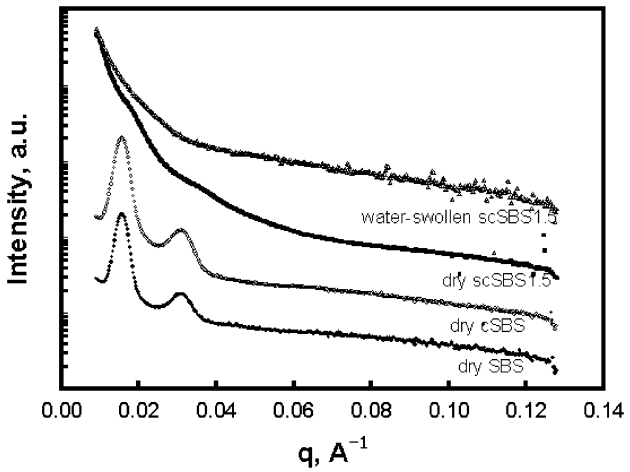

Figure 4. SAXS profiles of dry SBS, dry cSBS, dry scSBS1.5, and water-swollen scSBS1.5 samples.

lattice result in relative q values of 1, $3^{1/2}$, $4^{1/2}$, $7^{1/2}$, $9^{1/2}$, $12^{1/2}$, and so on.[39−41] The sequence of reflections in Figure 4 is in accordance with the assumption of a hexagonal packing of cylinders. The intercylinder distance, a, is given by[39−41]

$$a = \frac{2\pi}{q^*}\sqrt{\frac{4}{3}} \tag{2}$$

where q^* is the q position of the first maximum. Then the cylinder diameter, d, can be determined by

$$d = a\sqrt{\frac{2\sqrt{3}\phi_{PS}}{\pi}} \tag{3}$$

where ϕ_{PS} is the volume fraction of the microdomain. The intercylinder distance and cylinder diameter for the dry SBS film were calculated using $q^* = 0.0156$ Å^{-1} and $\phi_{PS} = 0.27$ as specified by the manufacturer and found to be 460 Å and 240 Å, respectively. Figure 4 shows that the intercylinder distance for the cSBS sample is almost the same as that of the pristine SBS film. The cylindrical morphology of the triblock copolymer is maintained with cross-linking, but it starts to disappear with increasing sulfonation. However, this cylindrical morphology is maintained for each sulfonated film up to scSBS1.5. The spatial arrangements of the microdomains for the water-swollen scSBS1.5 membrane are indistinct.

TEM is able to provide more localized information about selected areas of block copolymers (usually in the range of a few square micrometers) than SAXS, which probes a large sample volume. Figure 5 shows TEM micrographs of cSBS and sulfonated cSBS samples microtomed in arbitrarily chosen directions. The dark region corresponds to the PB phase selectively stained with OsO_4, and the bright region is associated with the unstained PS microdomain. These micrographs are in agreement with a microdomain arrangement consisting of hexagonal packing of cylinders, and this is consistent with the corresponding SAXS profile which exhibits a $\sqrt{3}$ Bragg's peak (Figure 4) and with previous observations.[26,42] However, it was not possible with TEM to observe any specific structural domains for highly sulfonated scSBS, e.g., for scSBS2, as was also the case for the SAXS measurements.

Ionic Channel Formation and Proton Conductivity. Proton transport occurs through the ionic channels of the proton-exchange membranes. Micro- or nanophase separation between the hydrophilic proton exchange sites and the hydrophobic domain, as found in the Nafion or sSEBS membranes, can provide ionic channels for proton transport. In the case of the SBS triblock copolymer, a microphase-separated structure arises because of the delicate balance between minimizing the unfavorable interaction energy between the incompatible blocks and maximizing the conformational entropy of the system. The characteristic size of the microphase-separated domains is known to be of the order of 10 nm.

In this work, the importance of the presence of ionic channels in the membrane was studied by comparing the structures and proton conductivities of SBR and SBS membranes. According to the SAXS and TEM results, the SBS membrane has polystyrene cylindrical domains that are dispersed as a hexagonal array in the polybutadiene matrix, and this structure persists after cross-linking. The polystyrene phase is substituted with hydrophilic sulfonated sites, providing nanosize proton transport channels, and the overall structure of the channels is maintained by the cross-linkages obtained before sulfonation. The structure becomes less distinct on sulfonation but still maintains its microphase separation.

In the case of the SBR membrane, no specific structural domains were detected in the pristine, cross-linked, or sulfonated SBR membranes. Thus, it is expected that there are no specific ionic channels for proton transport in scSBR.

As described above, the degrees of swelling of the SBR and SBS membranes are similar for a given degree of sulfonation. However, the proton conductivity of the

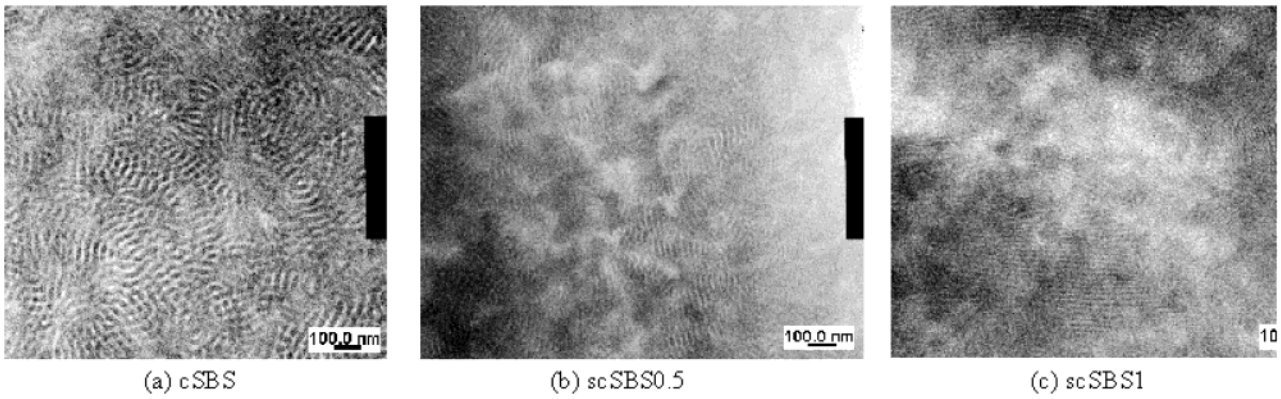

Figure 5. TEM micrographs of cSBS, scSBS0.5, and scSBS1 samples.

Scheme 2

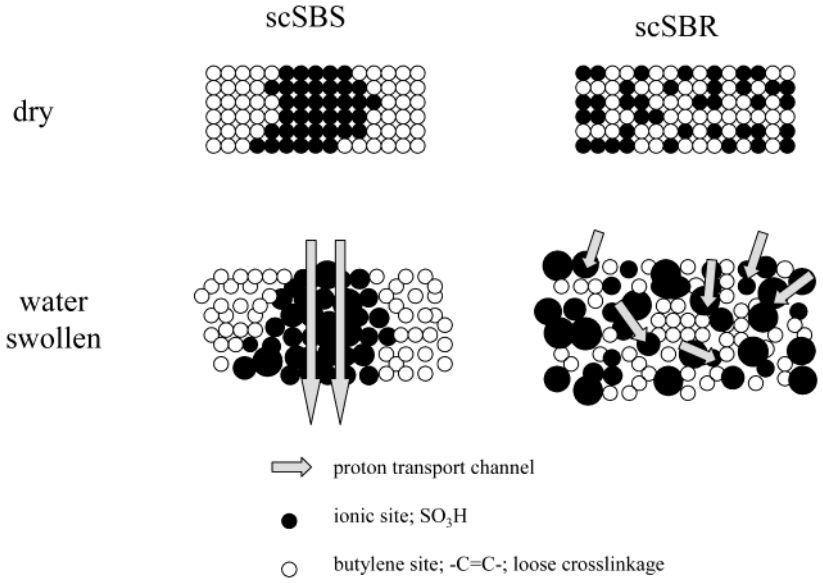

scSBS membrane is 3 orders of magnitude higher than that of the scSBR membrane. The similar degree of swelling implies that ionic clusters form and become swollen in water to almost the same extent in the two membranes. In the case of the scSBR membrane, the formed clusters occur at isolated sites, i.e., they may not be interconnected; interconnection is crucial to proton conduction. On the other hand, the scSBS membrane has interconnected ionic clusters, i.e., ionic channels, resulting in higher proton conductivity. On the basis of these results, the morphology and transport mechanisms can be deduced and are schematically drawn in Scheme 2.

Fixation of Ionic Channels and Its Effects on Methanol Permeability. It is known that methanol primarily permeates through hydrophilic ionic channels and that protons dominantly permeate by hopping between ionic sites. Thus, the methanol permeability strongly depends on the cross-sectional size of the ionic channels, but the proton conductivity does not. It is therefore expected that the methanol permeability should be decreased by reducing the size of the ionic channels while the proton conductivity should be virtually unchanged.

The control of the size of ionic channels has previously been attempted by phase separation and fixing of the hydrophobic matrix, and the effect of ionic channel size on methanol transport was then investigated by comparing cross-linked (scSBS) and non-cross-linkable (sSEBS) block copolymer membranes, both of which have microdomain structure.[18,31,43] The intercylinder distance and cylinder diameter for the dried sSEBS membrane were calculated from SAXS measurements using the values $q^* = 0.0167$ Å^{-1} and $\phi_{PS} = 0.25$, as specified by the manufacturer, and found to be 430 Å and 230 Å, respectively;[31] these values are comparable to those of the dried scSBS membrane. From the SAXS profiles for sSEBS membranes in the dried and water-swollen states, it can be seen that the membrane maintains its structure after swelling, but that the value of q^* moves to a lower scattering angle of 0.0106 Å^{-1} for the water-swollen state (see Figure 6). This means that the cylindrical structure is maintained on swelling but that the interdomain spacing increases by approximately 680 Å, as does the cylindrical diameter,

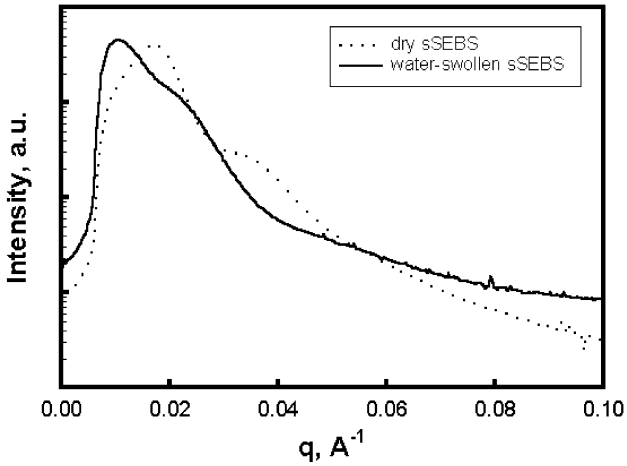

Figure 6. SAXS profiles of dry and water-swollen sSEBS films.

representing a significance increase in the size of the ionic channels. This significant swelling occurs because there is no permanent fixing of the structure in linear sSEBS membranes, as demonstrated by the high water uptake content values. On the other hand, for the case of cross-linked membranes, the domain structure of the scSBS membrane became complicated because of the additional driving force for the phase separation; the ionic interaction with the substitution of sulfonic sites of the channel structure was added on the original immiscibility of each block. As a result, the structure of the scSBS membrane becomes indistinct on swelling, but the permanent cross-linkages prevent complete disentanglement and reduce its swellability.

When the scSBS2 and sSEBS membranes are compared, the degree of sulfonation and the proton conductivity are compatible, but the methanol permeability of the scSBS2 is 2 orders of magnitude lower than that of the sSEBS. This result suggests the importance of the ionic channel size in determining methanol permeability, as summarized in Table 1. Therefore, it is possible to decrease the methanol permeability while maintaining an almost unchanged proton conductivity by reducing the ionic channel size and fixing the hydrophobic matrix with cross-linkages.

On this basis, it can be concluded that a new proton-exchange membrane for DMFCs has been successfully prepared, which has a methanol permeability more than 1 order of magnitude less than that of Nafion yet comparable proton conductivity. The performance comparison can be quantified further by defining a ratio of proton ion conductivity to methanol permeability, Φ; the higher this ratio, the better the membrane performance in fuel cells.[44] The ratio for the Nafion 117 membrane—which is at present the most widely utilized membrane in liquid-feed methanol fuel cells—is also included for comparison in Table 1. It is noteworthy that Φ for scSBS2 is higher than that of Nafion by 1 order of magnitude.

4. Conclusions

Fixed-structure proton-exchange membranes were successfully prepared by cross-linking and sulfonating SBS block copolymers. The scSBS membrane exhibits a methanol permeability of 8.1×10^{-8} cm^2/s, more than 30 times smaller than that of Nafion, with only a small reduction in proton conductivity. This is the advantage of fixing the membrane structure; fixation of the microphase-separated structure reduces the swellability of the chains and therefore significantly blocks methanol transport through the ionic channels, a feature that is particularly attractive for its prospective use as a proton-exchange membrane in direct methanol fuel cells.

The significance of ionic channel formation, i.e., the formation of interconnected ion clusters, was deduced by comparing the characteristics of SBR and SBS copolymers with different morphologies. It was concluded that their proton conductivity depends on both their degree of sulfonation and the formation of ionic channels. However, the degree of swelling depends only on the extent of sulfonation. Since methanol primarily permeates the membranes along the ionic channels, it was expected that limiting the ionic channel size would severely limit the methanol permeability but would not affect the proton conductivity. The channel size was fixed by cross-linking the hydrophobic matrix; the expected effect of this on methanol permeability was confirmed by comparing the ionic conductivities and methanol permeabilities of cross-linked scSBS and non-cross-linkable sSEBS membranes.

Acknowledgment. Support for this work was provided by the Korea Research Council of Fundamental Science and Technology and by the Ministry of Science and Technology of Korea (Creative Research Initiatives Program) and by Korea Energy Management Corp. (2002NFC03P010000). K.J.I. acknowledges the financial support provided by the Research Center for Advanced Mineral Composite Products by KOSEF in Kangwon National University. This work benefited from the use of the Synchrotron source 4C1 SAXS beamline at the Pohang Accelerator Laboratory (PAL) and of the Korea and SAXS instruments with Cu Kα radiation at the National Instrumentation Center for Environment Management (NICEM).

References and Notes

(1) For example: Böddeker, K. W.; Peinemann, K.-V.; Nunes, S. P. *J. Membr. Sci.* **2001**, *185*, 1.
(2) Ravikumar, M. K.; Shukla, A. K. *J. Electrochem. Soc.* **1996**, *143*, 2601.
(3) Küver, A.; Vielstich, W. *J. Power Sources* **1998**, *74*, 211.
(4) Kreuer, K. D.; Weppner, W.; Rabenau, A. *Angew. Chem., Int. Ed. Engl.* **1982**, *21*, 208.
(5) Pu, C.; Huang, W.; Ley, K. L.; Smotkin, E. S. *J. Electrochem. Soc.* **1995**, *142*, 119.
(6) Burstein, G. T.; Barnett, C. J.; Kucernak, A. R.; Williams, K. R. *Catal. Today* **1998**, *38*, 425.
(7) Tricoli, V.; Carretta, N.; Bartolozzi, M. *J. Electrochem. Soc.* **2000**, *147*, 1286.
(8) Kerres, J.; Cui, W.; Disson, R.; Neubrand, W. *J. Membr. Sci.* **1998**, *139*, 211.
(9) Weiss, R. A.; Sen, A.; Pottick, L. A.; Willis, C. L. *Polym. Commun.* **1990**, *31*, 220.
(10) Weiss, R. A.; Sen, A.; Willis, C. L.; Pottick, L. A. *Polymer* **1991**, *32*, 1867.
(11) Sheikh-Ali, B. M.; Wnek, G. E. U.S. Patent, 6,110,616, 2000.
(12) Ehrenberg, S. G.; Serpico, J. M.; Wnek, G. E.; Rider, J. N. U.S. Patent, 5,679,482, 1997.
(13) Ehrenberg, S. G.; Serpoci, J. M.; Wnek, G. E.; Rider, J. N. U.S. Patent, 5,468,574, 1995.
(14) Mokrini, A.; Acosta, J. L. *Polymer* **2001**, *42*, 9.
(15) Ehrenberg, S. G.; Serpico, J. M.; Sheikh-Ali, B. M.; Tangredi, T. N.; Zador, E.; Wnek, G. E. In Savadogo, O., Roberge, P. R., Eds.; Proceedings of the second international symposium on new materials for fuel cell and modern battery systems. Montreal Canada, 1997; p 828.
(16) Wnek, G. E.; Rider, J. N.; Serpico, J. M.; Einset, A. G. Proceedings of the First International Symposium on Proton Conducting Membrane Fuel Cells. *Electrochem. Soc. Proc.* **1995**, 247.
(17) Grot, W. *Chem. Ing. Technol.* **1978**, *50*, 299.
(18) Weiss, R. A.; Sen, A.; Pottick, L. A.; Willis, C. L. *Polymer* **1991**, *32*, 2785.
(19) Nishide, M.; Eisenberg, A. *Macromolecules* **1996**, *29*, 1507.
(20) Green, G. E.; Stark, B. P.; Zahir, S. A. *J. Macromol. Sci., Rev. Macromol. Chem.* **1982**, *C21*, 187.
(21) Puskas, J. E.; Kennedy, G. J. P. *J. Macromol. Sci., Chem.* **1991**, *A28*, 65. Crivello, J. V.; Yang, B. *J. Macromol. Sci., Chem.* **1994**, *A31*, 517.
(22) Le Xuan, H.; Decker, C. *J. Polym. Sci., Polym. Chem. Ed.* **1993**, *31*, 769.
(23) Ellenstein, S. M.; Lee, S. A.; Palit, T. K. In *Radiation Curing in Polymer Science and Technology*; Fouassier, J. P., Rabek, J. F., Eds.; Elsevier Applied Science: London, 1993; Vol. 4.
(24) Decker, C.; Viet, T. N. T. *Macromol. Chem. Phys.* **1999**, *200*, 358.
(25) Dakin, V. *Radiat. Phys. Chem.* **1995**, *45*, 715.
(26) Zhang, Q.; Tsui, O. K. C.; Du, B.; Zhang, F.; Tang, T.; He, T. *Macromolecules* **2000**, *33*, 9561.
(27) Verbrugge, M. W. *J. Electrochem. Soc.* **1989**, *136*, 417.
(28) Vargas, M. A.; Vargas, R. A.; Mellander, B.-E. *Electrochim. Acta* **1999**, *44*, 4227.
(29) Vargas, R. A.; García, A.; Vargas, M. A. *Electrochim. Acta* **1998**, *43*, 1271.
(30) Fontanella, J. J.; Wintersgill, M. C.; Wainrght, J. S.; Savinell, R. F.; Litt, M. *Electrochim. Acta* **1998**, *43*, 1289.
(31) Won, J.; Choi, S. W.; Kang, Y. S.; Ha, H. Y.; Oh, I.-H.; Kim, H. S.; Kim, K. T.; Jo, W. H. *J. Membr. Sci.*, **2003**, *214*, 245.
(32) Tricoli, V. *J. Electrochem. Soc.* **1998**, *145*, 3798.
(33) Carretta, N.; Tricoli, V.; Picchioni, F. *J. Membr. Sci.* **2000**, *166*, 189.
(34) Pivovar, B. S.; Wang, Y.; Cussler, E. L. *J. Membr. Sci.* **1999**, *154*, 155.
(35) Xingzhou, H.; Zubo, L. *Polym. Degrad. Stab.* **1995**, *48*, 99.
(36) De Paoli, M.-A. *Eur. Polym. J.* **1983**, *19*, 761.
(37) Zchocke, P.; Quellmalz, D. *J. Membr. Sci.* **1985**, *22*, 325.
(38) Hinatsu, J. T.; Mizuhata, M.; Takenaka, H. *J. Electrochem. Soc.* **1994**, *141*, 1493.
(39) Storey, R. F.; Baugh, D. W., III *Polymer* **2000**, *41*, 3205.
(40) Heck, B.; Arends, P.; Ganter, M.; Kressler, J.; Stühn, B. *Macromolecules* **1997**, *30*, 4559.
(41) Sakurai, S.; Kawada, H.; Hashimoto, T.; Fetters, L. J. *Macromolecules* **1993**, *26*, 5796.
(42) Wang, C. *Macromolecules*, **2001**, *34*, 9006.
(43) Lu, X.; Steckle, W. P.; Weiss, R. A. *Macromolecules* **1993**, *26*, 6525.
(44) Carretta, N.; Tricoli, V.; Picchioni, F. *J. Membr. Sci.* **2000**, *166*, 189.

MA034014B